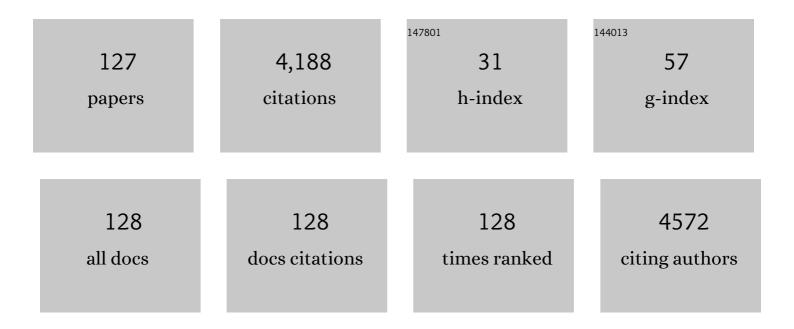
List of Publications by Year in descending order

Source: https://exaly.com/author-pdf/4730121/publications.pdf Version: 2024-02-01



#	Article	IF	CITATIONS
1	Single-atom Rh/N-doped carbon electrocatalyst for formic acid oxidation. Nature Nanotechnology, 2020, 15, 390-397.	31.5	420
2	Graphene nanosheets as novel adsorbents in adsorption, preconcentration and removal of gases, organic compounds and metal ions. Science of the Total Environment, 2015, 502, 70-79.	8.0	196
3	Enantioselective Total Synthesis of Lycopodine. Journal of the American Chemical Society, 2008, 130, 9238-9239.	13.7	151
4	Photocatalytic, Phosphoranyl Radical-Mediated N–O Cleavage of Strained Cycloketone Oximes. Organic Letters, 2019, 21, 2658-2662.	4.6	130
5	Novel S, N-doped carbon quantum dot-based "off-on" fluorescent sensor for silver ion and cysteine. Talanta, 2018, 180, 300-308.	5.5	121
6	Visible-Light-Driven, Radical-Triggered Tandem Cyclization of <i>o</i> -Hydroxyaryl Enaminones: Facile Access to 3-CF ₂ /CF ₃ -Containing Chromones. Organic Letters, 2017, 19, 146-149.	4.6	99
7	Synthesis of Pyrrolo(spiro-[2.3′]-oxindole)-spiro-[4.3″]-oxindole via 1,3-Dipolar Cycloaddition of Azomethine Ylides with 3-Acetonylideneoxindole. Journal of Organic Chemistry, 2013, 78, 11577-11583.	3.2	90
8	Photoinduced Singleâ€Electron Transfer as an Enabling Principle in the Radical Borylation of Alkenes with NHC–Borane. Angewandte Chemie - International Edition, 2020, 59, 6706-6710.	13.8	89
9	<i>N</i> -(<i>p</i> -Dodecylphenylsulfonyl)-2-pyrrolidinecarboxamide: A Practical Proline Mimetic for Facilitating Enantioselective Aldol Reactions. Organic Letters, 2008, 10, 4649-4652.	4.6	80
10	Advancement in the chemical analysis and quality control of flavonoid in Ginkgo biloba. Journal of Pharmaceutical and Biomedical Analysis, 2015, 113, 212-225.	2.8	79
11	Simultaneous In Situ Extraction and Fabrication of Surface-Enhanced Raman Scattering Substrate for Reliable Detection of Thiram Residue. Analytical Chemistry, 2018, 90, 13647-13654.	6.5	79
12	Asymmetric Construction of Nitrogen-Containing [2.2.2] Bicyclic Scaffolds Using N-(p-Dodecylphenylsulfonyl)-2-pyrrolidinecarboxamide. Journal of Organic Chemistry, 2009, 74, 5151-5156.	3.2	78
13	Highly Stereoselective and Scalable <i>anti</i> -Aldol Reactions Using <i>N</i> -(<i>p</i> -Dodecylphenylsulfonyl)-2-pyrrolidinecarboxamide: Scope and Origins of Stereoselectivities. Journal of Organic Chemistry, 2010, 75, 7279-7290.	3.2	74
14	Development of an Enantioselective Route toward the <i>Lycopodium</i> Alkaloids: Total Synthesis of Lycopodine. Journal of Organic Chemistry, 2010, 75, 4929-4938.	3.2	69
15	Synthesis of All-Carbon, Quaternary Center-Containing Cyclohexenones through an Organocatalyzed, Multicomponent Coupling. Organic Letters, 2010, 12, 3108-3111.	4.6	66
16	Interrogation of spatial metabolome of <i>Ginkgo biloba</i> with highâ€resolution matrixâ€assisted laser desorption/ionization and laser desorption/ionization mass spectrometry imaging. Plant, Cell and Environment, 2018, 41, 2693-2703.	5.7	65
17	Fetal bovine serum influences the stability and bioactivity of resveratrol analogues: A polyphenol-protein interaction approach. Food Chemistry, 2017, 219, 321-328.	8.2	61
18	Nitrogen-doped carbon dots rapid and selective detection of mercury ion and biothiol and construction of an IMPLICATION logic gate. Talanta, 2019, 194, 554-562.	5.5	59

#	Article	IF	CITATIONS
19	Rapid and visual detection of aflatoxin B1 in foodstuffs using aptamer/G-quadruplex DNAzyme probe with low background noise. Food Chemistry, 2019, 271, 581-587.	8.2	58
20	Visible-Light-Induced External Radical-Triggered Annulation To Access CF ₂ -Containing Benzoxepine Derivatives. Organic Letters, 2018, 20, 1363-1366.	4.6	55
21	Structure, synthesis, biosynthesis, and activity of the characteristic compounds from <i>Ginkgo biloba</i> L Natural Product Reports, 2022, 39, 474-511.	10.3	54
22	A gas-diffusion microfluidic paper-based analytical device (μPAD) coupled with portable surface-enhanced Raman scattering (SERS): facile determination of sulphite in wines. Analyst, The, 2016, 141, 5511-5519.	3.5	49
23	Enantioselective Mannich Reactions with the Practical Proline Mimetic N-(p-Dodecylphenyl-sulfonyl)-2-pyrrolidinecarboxamide. Journal of Organic Chemistry, 2009, 74, 2246-2249.	3.2	46
24	Separation of polyphenols from leaves of Malus hupehensis (Pamp.) Rehder by off-line two-dimensional High Speed Counter-Current Chromatography combined with recycling elution mode. Food Chemistry, 2015, 186, 139-145.	8.2	44
25	Synthesis of Multi-Au-Nanoparticle-Embedded Mesoporous Silica Microspheres as Self-Filtering and Reusable Substrates for SERS Detection. ACS Applied Materials & Interfaces, 2017, 9, 42156-42166.	8.0	44
26	Photocatalytic C–F Bond Borylation of Polyfluoroarenes with NHC-boranes. Organic Letters, 2020, 22, 1742-1747.	4.6	43
27	Highly Enantioselective Construction of Polycyclic Spirooxindoles by Organocatalytic 1,3â€Dipolar Cycloaddition of 2â€Cyclohexenone Catalyzed by Prolineâ€Sulfonamide. European Journal of Organic Chemistry, 2014, 2014, 5700-5704.	2.4	40
28	In situ synthesis of gold nanoparticles on pseudo-paper films as flexible SERS substrate for sensitive detection of surface organic residues. Talanta, 2019, 197, 225-233.	5.5	38
29	Nitrogen-doped carbon quantum dots as a fluorescent probe to detect copper ions, glutathione, and intracellular pH. Analytical and Bioanalytical Chemistry, 2018, 410, 7701-7710.	3.7	37
30	Additive-assisted regioselective 1,3-dipolar cycloaddition of azomethine ylides with benzylideneacetone. Beilstein Journal of Organic Chemistry, 2014, 10, 352-360.	2.2	35
31	Effect of varying NaCl doses on flavonoid production in suspension cells of Ginkgo biloba: relationship to chlorophyll fluorescence, ion homeostasis, antioxidant system and ultrastructure. Acta Physiologiae Plantarum, 2014, 36, 3173-3187.	2.1	34
32	Visibleâ€Lightâ€Promoted Synthesis of 1,4â€Dicarbonyl Compounds via Conjugate Addition of Aroyl Chlorides. Chemistry - an Asian Journal, 2018, 13, 271-274.	3.3	34
33	Visible-Light-Induced, Catalyst-Free Radical Cross-Coupling Cyclization of <i>N</i> -Allylbromodifluoroacetamides with Disulfides or Diselenides. Journal of Organic Chemistry, 2020, 85, 5670-5682.	3.2	34
34	<i>L</i> -Pyroglutamic Sulphonamide as Hydrogen-Bonding Organocatalyst: Enantioselective Diels–Alder Cyclization to Construct Carbazolespirooxindoles. Journal of Organic Chemistry, 2017, 82, 6441-6449.	3.2	32
35	Core-shell-satellite microspheres-modified glass capillary for microsampling and ultrasensitive SERS spectroscopic detection of methotrexate in serum. Sensors and Actuators B: Chemical, 2018, 275, 267-276.	7.8	32
36	Visible-Light-Driven, Photoredox-Catalyzed Cascade of <i>ortho-</i> Hydroxycinnamic Esters To Access 3-Fluoroalkylated Coumarins. Journal of Organic Chemistry, 2019, 84, 7480-7487.	3.2	31

#	Article	IF	CITATIONS
37	Selenocyanobenziodoxolone: a practical electrophilic selenocyanation reagent and its application for solid-state synthesis of α-carbonyl selenocyanates. Organic Chemistry Frontiers, 2019, 6, 1967-1971.	4.5	30
38	Simultaneous <i>In Situ</i> Extraction and Self-Assembly of Plasmonic Colloidal Gold Superparticles for SERS Detection of Organochlorine Pesticides in Water. Analytical Chemistry, 2021, 93, 4657-4665.	6.5	30
39	Visible-Light-Driven Sulfonation of α-Trifluoromethylstyrenes: Access to Densely Functionalized CF ₃ -Substituted Tertiary Alcohol. Organic Letters, 2021, 23, 6558-6562.	4.6	30
40	Accurate analysis of ginkgolides and their hydrolyzed metabolites by analytical supercritical fluid chromatography hybrid tandem mass spectrometry. Journal of Chromatography A, 2015, 1388, 251-258.	3.7	29
41	Photocatalytic reductive radical–radical coupling of <i>N</i> , <i>N</i> â€2-cyclicazomethine imines with difluorobromo derivatives. Chemical Communications, 2019, 55, 2712-2715.	4.1	29
42	Photocatalytic Hydroacylation of Alkenes by Directly Using Acyl Oximes. Journal of Organic Chemistry, 2020, 85, 11989-11996.	3.2	29
43	<i>>O</i> -Perfluoropyridin-4-yl Oximes: Iminyl Radical Precursors for Photo- or Thermal-Induced N–O Cleavage in C(sp ²)–C(sp ³) Bond Formation. Journal of Organic Chemistry, 2020, 85, 3538-3547.	3.2	29
44	Visible-Light-Induced, Palladium-Catalyzed 1,4-Difunctionalization of 1,3-Dienes with Bromodifluoroacetamides. Organic Letters, 2022, 24, 924-928.	4.6	29
45	Metal-free visible-light-initiated direct C3 alkylation of quinoxalin-2(1 <i>H</i>)-ones and coumarins with unactivated alkyl iodides. Green Chemistry, 2022, 24, 858-863.	9.0	29
46	Systematic and efficient separation of 11 compounds from Rhizoma Chuanxiong via counter-current chromatography–solid phase extraction–counter-current chromatography hyphenation. Journal of Chromatography A, 2014, 1364, 204-213.	3.7	28
47	Acidâ€Relayed Organocatalytic <i>exo</i> â€Diels–Alder Cycloaddition of Cyclic Enones with 2â€Vinylâ€l <i>H</i> â€indoles. European Journal of Organic Chemistry, 2016, 2016, 1264-1268.	2.4	28
48	Photoredox-Catalyzed Reductive Dimerization of Isatins and Isatin-Derived Ketimines: Diastereoselective Construction of 3,3′-Disubstituted Bisoxindoles. Journal of Organic Chemistry, 2017, 82, 3895-3900.	3.2	28
49	Organocatalytic, Enantioselective, Polarity-Matched Ring-Reorganization Domino Sequence Based on the 3-Oxindole Scaffold. Organic Letters, 2019, 21, 2166-2170.	4.6	28
50	<scp>l</scp> -Pyroglutamic Acid-Modified CdSe/ZnS Quantum Dots: A New Fluorescence-Responsive Chiral Sensing Platform for Stereospecific Molecular Recognition. Analytical Chemistry, 2020, 92, 12040-12048.	6.5	28
51	Synthesis of functionalized chromones via organocatalysis. Tetrahedron, 2014, 70, 9314-9320.	1.9	26
52	Selectfluor-Triggered Tandem Cyclization of <i>o</i> -Hydroxyarylenaminones To Access Difluorinated 2-Amino-Substituted Chromanones. Journal of Organic Chemistry, 2017, 82, 9837-9843.	3.2	26
53	Improved enantioseparation via the twin-column based recycling high performance liquid chromatography. Journal of Chromatography A, 2014, 1363, 236-241.	3.7	25
54	Diastereoselective Intramolecular [3 + 2]-Annulation of Donor–Acceptor Cyclopropane with Imine-Assembling Hexahydropyrrolo[3,2 <i>-c</i>]quinolinone Scaffolds. Journal of Organic Chemistry, 2016, 81, 11185-11194.	3.2	25

#	Article	IF	CITATIONS
55	In situ fabrication of label-free optical sensing paper strips for the rapid surface-enhanced Raman scattering (SERS) detection of brassinosteroids in plant tissues. Talanta, 2017, 165, 313-320.	5.5	25
56	<i>O</i> -Perhalopyridin-4-yl Hydroxylamines: Amidyl-Radical Generation Scaffolds in Photoinduced Direct Amination of Heterocycles. Organic Letters, 2021, 23, 1643-1647.	4.6	25
57	Proline sulphonamide-catalysed Yamada–Otani condensation: reaction development, substrate scope and scaffold reactivity. Organic and Biomolecular Chemistry, 2012, 10, 4851.	2.8	24
58	Highly stereoselective construction of novel dispirooxindole–imidazolidines via self-1,3-dipolar cyclization of ketimines. Organic and Biomolecular Chemistry, 2015, 13, 7907-7910.	2.8	24
59	Discovery of temperature-dependent, autoinductive reversal of enantioselectivity: palladium-mediated [3+3]-annulation of 4-hydroxycoumarins. Chemical Communications, 2017, 53, 4441-4444.	4.1	23
60	Palladium-catalysed ring-opening [3 + 2]-annulation of spirovinylcyclopropyl oxindole to diastereoselectively access spirooxindoles. Organic and Biomolecular Chemistry, 2019, 17, 103-107.	2.8	23
61	Construction of Bispirooxindole Heterocycles via Palladium-Catalyzed Ring-Opening Formal [3 + 2]-Cycloaddition of Spirovinylcyclopropyl Oxindole and 3-Oxindole Derivatives. Journal of Organic Chemistry, 2019, 84, 2297-2306.	3.2	23
62	Photoredox-Catalyzed Cascade of <i>o-</i> Hydroxyarylenaminones to Access 3-Aminated Chromones. Journal of Organic Chemistry, 2022, 87, 1477-1484.	3.2	23
63	Regioselectivity-Tunable Self-1,3-Dipolar [3+3] Cyclizations of Azomethine Ylides To Assemble Dispirooxindole-piperazines. Journal of Organic Chemistry, 2015, 80, 11573-11579.	3.2	22
64	Development of a "Dual Gates―Locked, Target-Triggered Nanodevice for Point-of-Care Testing with a Glucometer Readout. ACS Sensors, 2019, 4, 968-976.	7.8	22
65	Electrochemical heterodifunctionalization of α-CF ₃ alkenes to access α-trifluoromethyl-β-sulfonyl tertiary alcohols. Chemical Communications, 2021, 57, 8969-8972.	4.1	22
66	Amide-assisted intramolecular [3+2] annulation of cyclopropane ring-opening: a facile and diastereoselective access to the tricyclic core of (±)-scandine. Chemical Communications, 2016, 52, 2177-2180.	4.1	21
67	Sensitive surface enhanced Raman spectroscopy (SERS) detection of methotrexate by core-shell-satellite magnetic microspheres. Talanta, 2017, 171, 152-158.	5.5	21
68	Rapid screening and identification of antioxidants in the leaves of <i>Malus hupehensis</i> using offâ€line twoâ€dimensional HPLC–UV–MS/MS coupled with a 1,1′â€diphenylâ€2â€picrylhydrazyl assay. Jo Separation Science, 2018, 41, 2536-2543.	ouznal of	21
69	Intelligent Platform for Simultaneous Detection of Multiple Aminoglycosides Based on a Ratiometric Paper-Based Device with Digital Fluorescence Detector Readout. ACS Sensors, 2019, 4, 3283-3290.	7.8	21
70	Diversity-driven and facile 1,3-dipolar cycloaddition to access dispirooxindole-imidazolidine scaffolds. Organic and Biomolecular Chemistry, 2017, 15, 8705-8708.	2.8	20
71	Photocatalytic intermolecular <i>anti</i> -Markovnikov hydroamination of unactivated alkenes with <i>N</i> -hydroxyphthalimide. Organic Chemistry Frontiers, 2021, 8, 273-277.	4.5	20
72	Photocatalytic Cyclization/Defluorination Domino Sequence to Access 3-Fluoro-1,5-dihydro-2 <i>H</i> -pyrrol-2-one Scaffold. Organic Letters, 2021, 23, 4754-4758.	4.6	20

#	Article	IF	CITATIONS
73	Recent progress in the nitration of arenes and alkenes. Organic and Biomolecular Chemistry, 2021, 19, 4835-4851.	2.8	20
74	EnantioselectiveAldol Reaction Between Isatins and Cyclohexanone Catalyzed by Amino Acid Sulphonamides. Chirality, 2015, 27, 314-319.	2.6	19
75	Combining Metabolic Profiling and Gene Expression Analysis to Reveal the Biosynthesis Site and Transport of Ginkgolides in Ginkgo biloba L Frontiers in Plant Science, 2017, 8, 872.	3.6	19
76	Photoinduced Singleâ€Electron Transfer as an Enabling Principle in the Radical Borylation of Alkenes with NHC–Borane. Angewandte Chemie, 2020, 132, 6772-6776.	2.0	18
77	"Pomegranate-Like―Plasmonic Nanoreactors with Accessible High-Density Hotspots for in Situ SERS Monitoring of Catalytic Reactions. Analytical Chemistry, 2020, 92, 4115-4122.	6.5	18
78	Photochemical Organocatalytic Aerobic Cleavage of Câ∙€ Bonds Enabled by Charge-Transfer Complex Formation. Organic Letters, 2022, 24, 3920-3925.	4.6	18
79	Unraveling and Manipulating the Stereospecific Retro-Aldol Reaction in the Organocatalytic Asymmetric Aldol Reaction of Isatin and Cyclohexanone. Organic Letters, 2018, 20, 7535-7538.	4.6	17
80	Tunable photocatalytic oxysulfonylation and chlorosulfonylation of α-CF ₃ alkenes with sulfonyl chlorides. Organic Chemistry Frontiers, 2022, 9, 709-714.	4.5	17
81	Visible Light-Promoted Radical Relay Cyclization/C–C Bond Formation of <i>N</i> -Allylbromodifluoroacetamides with Quinoxalin-2(1 <i>H</i>)-ones. Journal of Organic Chemistry, 2021, 86, 17173-17183.	3.2	16
82	Visible-Light-Promoted Hydroxydifluoroalkylation of Alkenes Enabled by Electron Donor–Acceptor Complex. Organic Letters, 2021, 23, 9474-9479.	4.6	16
83	Phosphine-Mediated MBH-Type/Umpolung Addition Domino Sequence: Divergent Construction of Coumarins. Organic Letters, 2020, 22, 488-492.	4.6	14
84	A BHT-regulated chemoselective access to monofluorinated chromones. Tetrahedron, 2020, 76, 130833.	1.9	14
85	Proline Sulfonamide Based Organocatalysis: Better Late than Never. Synlett, 2010, 2010, 2827-2838.	1.8	13
86	Photoredox-catalyzed direct aminoalkylation of isatins: diastereoselective access to 3-hydroxy-3-aminoalkylindolin-2-ones analogues. Organic Chemistry Frontiers, 2018, 5, 1608-1612.	4.5	13
87	A Oneâ€Pot Ringâ€Opening/Ringâ€Closure Sequence for the Synthesis of Polycyclic Spirooxindoles. Chemistry - A European Journal, 2019, 25, 4673-4677.	3.3	13
88	<i>N</i> , <i>N</i> , <i>N</i> ', <i>N</i> '-Tetramethylethylenediamine-Enabled Photoredox-Catalyzed C–H Methylation of <i>N</i> -Heteroarenes. Journal of Organic Chemistry, 2021, 86, 11905-11914.	3.2	13
89	Enantioselective formal [3+2]-cycloadditions to access spirooxindoles bearing four contiguous stereocenters through synergistic catalysis. Chemical Communications, 2021, 57, 4456-4459.	4.1	13
90	Visible-Light-Induced, Palladium-Catalyzed Annulation of 1,3-Dienes to Construct Vinyl <i>N</i> -Heterocycles. Organic Letters, 2022, 24, 5407-5411.	4.6	13

#	Article	IF	CITATIONS
91	Straightforward Synthesis of 3-Selenocyanato-Substituted Chromones through Electrophilic Selenocyanation of Enaminones under Grinding Conditions. Synthesis, 2021, 53, 954-960.	2.3	12
92	Visible-light-promoted olefinic trifluoromethylation of enamides with CF ₃ SO ₂ Na. Organic and Biomolecular Chemistry, 2021, 19, 7475-7479.	2.8	12
93	Visible-Light-Driven, Photocatalyst-Free Cascade to Access 3-Cyanoalkyl Coumarins from ortho-Hydroxycinnamic Esters. Journal of Organic Chemistry, 2021, 86, 4245-4253.	3.2	12
94	Organocatalytic Enantioselective Conjugate Addition of Azlactones to Enolizable Linear and Cyclic Enones. Journal of Organic Chemistry, 2016, 81, 8001-8008.	3.2	11
95	Organocatalytic Asymmetric Allylic Alkylation of Morita–Baylis–Hillman Carbonates with Diethyl 2-Aminomalonate Assisted by In Situ Protection. Journal of Organic Chemistry, 2017, 82, 12202-12208.	3.2	11
96	Solvent-Minimized, Chromatography-Free, Diastereoselective Synthesis of Oxazolidine-Dispirooxindoles <i>via oxa</i> -1,3-Dipolar Cycloaddition of 3-Oxindole. Journal of Organic Chemistry, 2018, 83, 2948-2953.	3.2	10
97	Intramolecular hydrogen-bonding-assisted phosphine-catalysed [3 + 2] cyclisation of ynones with o-hydroxy/amino benzaldehydes. Organic and Biomolecular Chemistry, 2019, 17, 2187-2191.	2.8	10
98	Enantioselectivity-Switchable Organocatalytic [4 + 2]-Annulation to Access the Spirooxindole–Norcamphor Scaffold. Organic Letters, 2021, 23, 963-968.	4.6	10
99	Visible-Light-Promoted Cross-Coupling of <i>O</i> -Aryl Oximes and Nitrostyrenes to Access Cyanoalkylated Alkenes. Organic Letters, 2022, 24, 4640-4644.	4.6	10
100	Biphasic recognition enantioseparation of ofloxacin enantiomers by an aqueous two-phase system. Journal of Chemical Technology and Biotechnology, 2015, 90, 2234-2239.	3.2	9
101	Divergent Aerobic Oxidative Ringâ€Opening Cascades of Isatins with 1,2,3,4â€Tetrahydroisoquinoline. European Journal of Organic Chemistry, 2016, 2016, 5096-5101.	2.4	9
102	Organocatalytic Domino Entry to an Octahydroacridine Scaffold Bearing Three Contiguous Stereocenters. Journal of Organic Chemistry, 2018, 83, 12284-12290.	3.2	9
103	A phosphine-mediated domino sequence of salicylaldehyde with but-3-yn-2-one: rapid access to chromanone. Organic and Biomolecular Chemistry, 2020, 18, 8916-8920.	2.8	9
104	Photocatalyzed Defluorinative Dichloromethylation of α-CF ₃ Alkenes Using CHCl ₃ as the Radical Source. Journal of Organic Chemistry, 2023, 88, 6354-6363.	3.2	9
105	Enantioselective extraction of phenylsuccinic acid in aqueous two-phase systems based on acetone and β -cyclodextrin derivative: Modeling and optimization through response surface methodology. Journal of Chromatography A, 2016, 1467, 490-496.	3.7	8
106	Straightforward Synthesis of Novel Difluorinated 2â€Hydroxylâ€Substituted Dihydroquinolones Through Selectfluorâ€ŧriggered Annulation of 2â€Aminoarylenaminones. ChemistrySelect, 2018, 3, 9218-9221.	1.5	8
107	Cul-mediated benzannulation of (<i>ortho</i> -arylethynyl)phenylenaminones to assemble α-aminonaphthalene derivatives. Organic Chemistry Frontiers, 2021, 8, 3250-3254.	4.5	8
108	Phosphonium Ylide-Mediated Programmable Fluorination to Access Mono- and Difluoromethylarenes. Organic Letters, 2021, 23, 2538-2542.	4.6	8

#	Article	IF	CITATIONS
109	Facile oxidative cyclization to access C2-quaternary 2-hydroxy-indolin-3-ones: synthetic studies towards matemone. New Journal of Chemistry, 2017, 41, 11503-11506.	2.8	7
110	Unusual Ligandâ€ŧoâ€Metalâ€Ratioâ€Controlled Bidirectional Enantioselectivity in Pdâ€Catalysed [3+3]â€Annulation of Morita–Baylis–Hillman Acetate. European Journal of Organic Chemistry, 2017, 2017, 6961-6965.	2.4	7
111	A phosphine-catalysed one-pot domino sequence to access cyclopentene-fused coumarins. Organic and Biomolecular Chemistry, 2021, 19, 7074-7080.	2.8	7
112	Gold/scandium bimetallic relay catalysis of formal [5+2]- and [4+2]-annulations: access to tetracyclic indole scaffolds. Chemical Communications, 2021, 57, 13369-13372.	4.1	7
113	Facile Construction of Pyrrolo[1,2-a]indolenine Scaffold via DiaÂstereoselective [3+2] Annulation of Donor–Acceptor Cyclopropane with Indolenine. Synthesis, 2017, 49, 4292-4298.	2.3	6
114	Combining paired analytical metabolomics and common garden trial to study the metabolism and gene variation of <i>Ginkgo biloba</i> ÂL. cultivated varieties. RSC Advances, 2017, 7, 55309-55317.	3.6	5
115	Catalyst-controlled diastereoselective ring-opening formal [3+2]-cycloadditions of arylvinyl oxirane 2,2-diesters with cyclic N-sulfonyl imines. Science China Chemistry, 2020, 63, 785-791.	8.2	5
116	Integrating amino acid oxidase with photoresponsive probe: A fast quantitative readout platform of amino acid enantiomers. Talanta, 2021, 224, 121894.	5.5	5
117	TBN-triggered, manipulable annulations of <i>o</i> -hydroxyarylenaminones for divergent syntheses of oximinochromanones and oximinocoumaranones. Chemical Communications, 2021, 57, 12285-12288.	4.1	5
118	An organocatalytic enantioselective ring-reorganization domino sequence of methyleneindolinones with 2-aminomalonates. Organic Chemistry Frontiers, 2021, 8, 778-783.	4.5	4
119	Diastereoselectivityâ€&witchable Goldâ€Catalyzed Formal [3+2]â€Cycloadditions of <i>N</i> â€2,2,2â€Trifluoroethylisatin Ketimines with Yneâ^Enones. Chemistry - an Asian Journal, 2021, 16, 2435-2438.	3.3	4
120	Photoinduced Construction of a Benzothienopyridine- <i>S,S</i> -dioxide Framework Enabled by Polychloropyridyl Multifunctional Motifs. Journal of Organic Chemistry, 2022, 87, 4732-4741.	3.2	4
121	Organocatalytic domino sequence to asymmetrically access spirocyclic oxindole-α-methylene-γ-lactams. Tetrahedron, 2021, , 132163.	1.9	3
122	Intramolecular [3+2]-cycloaddition of salicylaldehydes-based cyclic azomethine imines to access novel tetrahydrochromeno[4,3-c]pyrazolo[1,2-a]pyrazol-9-ones. Tetrahedron, 2021, 83, 131992.	1.9	2
123	Unveiling the abnormal effect of temperature on enantioselectivity in the palladium-mediated decabonylative alkylation of MBH acetate. Organic Chemistry Frontiers, 2021, 8, 5058-5063.	4.5	2
124	Phosphine-Mediated Morita–Baylis–Hillman-Type/Wittig Cascade: Access to <i>E</i> -Configured 3-Styryl- and 3-(Benzopyrrole/furan-2-yl) Quinolinones. Journal of Organic Chemistry, 2022, 87, 974-984.	3.2	2
125	Programmable iodization/deuterolysis sequences of phosphonium ylides to access deuterated benzyl iodides and aromatic aldehydes. Chemical Communications, 2022, 58, 4215-4218.	4.1	1
126	Study on the Online Ink Testing with CCD Based on Calabro-Mercatucci Model. Advanced Materials Research, 2010, 174, 195-198.	0.3	0

#	Article	IF	CITATIONS
127	[3+2] vs [4+1] Annulation: Revisiting mechanism studies on phosphine-catalysed domino sequence of alkynoates and activated methylenes. Organic and Biomolecular Chemistry, 2022, , .	2.8	0